HHS Public Access

Author manuscript

Matrix Biol. Author manuscript; available in PMC 2018 January 01.

Published in final edited form as:

Matrix Biol. 2017 January ; 57-58: 347–365. doi:10.1016/j.matbio.2016.09.005.

Embryo Implantation Triggers Dynamic Spatiotemporal Expression of the Basement Membrane Toolkit During Uterine Reprogramming

Celestial R. Jones-Paris[a,b], **Sayan Paria**[b], **Taloa Berg**[b], **Juan Saus**[c,d], **Gautam Bhave**[e,f], **Bibhash C. Paria**[g,*], and **Billy G. Hudson**[a,*,c,e,f,h,i,j,k]

[a]Department of Pathology, Microbiology, and Immunology, Vanderbilt University Medical Center, Nashville, Tennessee, United States

[b]Aspirnaut, Vanderbilt University Medical Center, Nashville, Tennessee, United States

[c]Valencia University Medical School, Valencia, Spain

[d]Fibrostatin, SL, Valencia, Spain

[e]Division of Nephrology and Hypertension, Department of Medicine, Vanderbilt University Medical Center, Nashville, Tennessee, United States

[f]Center for Matrix Biology, Vanderbilt University Medical Center, Nashville, Tennessee, United States

[g]Division of Neonatology, Department of Pediatrics, Vanderbilt University Medical Center, Nashville, Tennessee, United States

[h]Department of Biochemistry, Vanderbilt University, Nashville, Tennessee, United States

[i]Department of Cell and Developmental Biology, Vanderbilt University Medical Center, Nashville, Tennessee, United States

[j]Vanderbilt Ingram Cancer Center, Nashville, Tennessee, United States

[k]Vanderbilt Institute of Chemical Biology Nashville, Tennessee, United States

Abstract

Basement membranes (BMs) are specialized extracellular scaffolds that influence behaviors of cells in epithelial, endothelial, muscle, nervous, and fat tissues. Throughout development and in response to injury or disease, BMs are fine-tuned with specific protein compositions, ultrastructure, and localization. These features are modulated through implements of the BM toolkit that is comprised of collagen IV, laminin, perlecan, and nidogen. Two additional proteins,

Corresponding authors: Billy G. Hudson (billy.hudson@Vanderbilt.Edu; mailing address: 1611 21st Ave South, B-3102 Medical Center North, Nashville, TN 37232-2372) and Bibhash C. Paria (bc.paria@Vanderbilt.Edu; mailing address: 2215 Garland Avenue, 1125 MRB IV/Light Hall, Nashville, TN 37232-0656).

*These authors contributed equally to this work

peroxidasin and Goodpasture antigen-binding protein (GPBP), have recently emerged as potential members of the toolkit. In the present study, we sought to determine whether peroxidasin and GPBP undergo dynamic regulation in the assembly of uterine tissue BMs in early pregnancy as a tractable model for dynamic adult BMs. We explored these proteins in the context of collagen IV and laminin that are known to extensively change for decidualization. Electron microscopic analyses revealed: 1) a smooth continuous layer of BM in between the epithelial and stromal layers of the preimplantation endometrium; and 2) interrupted, uneven, and progressively thickened BM within the pericellular space of the postimplantation decidua. Quantification of mRNA levels by qPCR showed changes in expression levels that were complemented by immunofluorescence localization of peroxidasin, GPBP, collagen IV, and laminin. Novel BM-associated and subcellular spatiotemporal localization patterns of the four components suggest both collective pericellular functions and distinct functions in the uterus during reprogramming for embryo implantation.

Keywords

Basement membrane; uterus; collagen IV; laminin; peroxidasin; Goodpasture antigen-binding protein (GPBP)

1. Introduction

Basement membranes (BMs) are complex extracellular scaffolds of proteins that circumscribe cell populations, modulate cell behaviors, and provide architectural and mechanical support to tissues [1,2]. Basement membranes play active roles in regulating tissue biology by being positioned adjacent to key cell types: 1) between the epithelial or endothelial cells and their underlying stromal compartment [3,4]; and 2) encapsulating cells such as myocytes [5–7], adipocytes [8,9], Schwann cells [10,11], and decidua cells [12–15]. These scaffolds activate signal transduction by directly interacting with transmembrane cell receptors, modulate paracrine signaling by regulating chemokine gradients and immobilizing growth factors, and establish tissue tension and integrity by bearing compression and expansion tissue forces [16–19]. Basement membranes are comprised of a group of proteins, including collagen IV, laminin, perlecan, and nidogen, that together are termed the BM toolkit [20–22]. Emerging concepts argue that BMs undergo dynamic physiological adaptation by being fine-tuned with specific composition and localization throughout the life of organisms [23–25], though the fundamental mechanisms remain unknown.

Two additional proteins have emerged as potential members of the toolkit: peroxidasin and Goodpasture antigen-binding protein (GPBP). Peroxidasin catalyzes the formation of sulfilimine crosslinks that reinforce collagen IV networks of BMs. The lack of these reinforcements led to early developmental disorders and dysfunction in several tissues and organisms [26–30]. However, observations of the dynamic distribution of peroxidasin in BMs is limited to development of *C. elegan* tissues [31] and cell lines [32], and has been implied in embryonic mouse tissues [29]. Extracellular GPBP was discovered through its binding to kidney BM [33] and has since been shown to bind major BM components laminin

and collagen IV [34,35]. Overexpression of GPBP in renal tissues is associated with collagen IV rearrangement and ultrastructure expansion of glomerular BM in immune complex-mediated pathogenesis in mice and humans [36,37]. Though peroxidasin and GPBP have been identified in several BMs, whether they undergo dynamic regulation in healthy adult tissues is unknown.

In the present study, we sought to determine whether peroxidasin and GPBP undergo dynamic regulation during distributional alterations of BM in an adapted physiological state. As a model system, we explored the BM dynamics that are known to occur in uterine tissue in early pregnancy. Embryo implantation triggers the endometrium to undergo rapid and extensive changes in cell populations and extracellular matrix (ECM) for development of the decidua, a cocoon-like tissue barrier between mother-embryo throughout pregnancy [38–42]. These changes include apoptosis of endometrial epithelial and endothelial cells, restriction of immune cell infiltration, and proliferation of mesenchymal stromal cells that differentiate into cells with select epithelial-like features, thus they are often referred to as epithelioid decidua cells (See Fig.1 and 2 in [43]). Studies of endometrial and decidual ECM show collagen IV and laminin change from limited localization underlying epithelial and endothelial cells to broad localization surrounding epithelioid cells throughout the mature decidua [12–15]. However, co-localization of these two proteins has not been examined upon the initial switch to decidua tissue, during the periimplantation period. Here, our findings further reveal that the uterus reacts to implantation by triggering the dynamic regulation of peroxidasin and GPBP, as well as collagen IV and laminin, with distinct spatiotemporal expression and localization patterns in uterine tissues, suggesting both individual and collective functions of these BM toolkit proteins.

2. Results

2.1. Ultrastructure of BM during decidua development

Previous studies of decidualization have established the mouse as a reliable species to model and examine changes to the uterus that occur in human pregnancy, even though some aspects of anatomy and timing differ between mice and humans [44–46]. In mice, endometrium epithelial and mesenchymal cell behaviors are altered upon the initiation of pregnancy through ovarian-derived hormones and cellular compartment cross-talk [47–50]. By day 4 of the 21-day term of pregnancy in mice, the uterus is conducive to blastocyst implantation and decidualization is triggered upon embryo attachment [51–53]. The majority of decidual tissue develops by day 7 of pregnancy and persists as the embryo grows and develops placenta that merges with the decidua for nutrient and waste exchange [38,54]. Although BMs have been observed in both pre-and post- implantation uterine tissues [12–15], little is known about the BM ultrastructure properties. In the present study, we investigated these properties by comparing the BM of the luminal epithelium of day 4 uteri (Fig.1A) and decidual zone of day 7 implantation sites (Fig. 1B) by transmission electron microscopy (TEM) that displays electron-dense layers of BMs called lamina densa.

In the endometrium on day 4 of pregnancy, a smooth and narrow layer of lamina densa was observed basal to cells of the luminal epithelium, but lamina densa was not within the stroma (Fig.1A)(See also Fig.3 in [43]). The location and structure of uterine epithelial

lamina densa displayed characteristics of basement membrane oriented basal to polarized cells with apical-lateral localized cell-cell junctions [3,55]. In the implantation site on day 7 of pregnancy, lamina densa was positioned within the pericellular space of cells throughout the decidua. However, lamina densa of the decidua had intermittent disruptions where cell-cell contacts and electron dense junctions were observed between cells (Fig.1B)(See also Fig.3 in [43]). These observations led us to further analyze characteristics of lamina densa of uterine luminal epithelium during periimplantation, also known as the window of implantation, and during the course of decidua development.

On day 5 of pregnancy, lamina densa of luminal epithelial cells adjacent to the attached blastocyst, appeared less uniform, morphologically frayed (Fig.1C) and slightly but significantly thicker (78 nm median, ± 55 nm standard deviation (SD), p-value < 0.001) (Fig.1D) compared to the BM of the day 4 luminal epithelium (65 nm median, ± 35 nm SD) (Fig.1D). Following implantation and decidualization on day 6 of pregnancy, lamina densa surrounding decidual cells was uneven and discontinuous, with variable widths but median thickness similar to that of day 5 (78 nm median, ± 45 nm SD) (Fig.1C–D). As the decidua matured, through days 7 and 8 of pregnancy, lamina densa presented with median thicknesses two-fold greater than preimplantation epithelial BM (120 nm and 138 nm medians, respectively) and greater variability of widths (±79 nm SD and ±111 nm SD, respectively) (Fig.1C–D). Pericellular gaps contained thickened lamina densa with some inclusion of fibrillar collagens in day 8 decidua (Fig.1C–D). Decidua adjacent to the day 8 embryo had little to no distinguishable BM (data not shown). In summary, through examination of ultrastructure changes, we found lamina densa associated with the development of the decidua accumulated progressively, initially presenting with a frayed and discontinuous morphology followed by a thickening in pericellular spaces around decidual cells.

2.2. Peroxidasin gene expression and protein localization with collagen IV in the uterus during early pregnancy

Recent studies have demonstrated the importance of peroxidasin in tissue development and integrity in several organisms [26,27,29,56]. However, the regulation of peroxidasin during pregnancy is unknown. To determine whether peroxidasin mRNA expression is altered in preparation for blastocyst attachment and/or during decidualization, we quantified expression levels of *Pxdn*, peroxidasin encoding gene, in whole uterine horns or implantation sites from day 1 through 8 of pregnancy. We found *Pxdn* expression was gradually reduced during days 1 through 3, and then increased markedly to near days 1 and 2 levels by day 5 of pregnancy. Following a significant drop in *Pxdn* levels between days 5 and 6 of pregnancy, levels remained unchanged from days 6–8 (Fig.2A). These results revealed *Pxdn* levels are up-regulated in the uterus during embryo attachment that occurs midway between days 4 and 5 of pregnancy in mice [57], but compartmentalized production was undetermined.

We, therefore, examined the localization of peroxidasin with collagen IV in the endometrium where robust tissue changes occur during early pregnancy. Using co-immunofluorescence, we determined if expression changes contributed to global distribution

or compartmentalized production of peroxidasin and if it was incorporated into BMs. We found peroxidasin localized to all areas of collagen IV in addition to some distinctive patterns. During the preimplantation period (days 1 through 4), peroxidasin localization was found in the BMs of epithelium and endothelium of the endometrium (Fig.2B, A'–D'). We observed patterns of short regions where peroxidasin appeared to concentrate along the lumen BM which was most pronounced on day 2 of pregnancy (Fig.2B, B'). Cytoplasmic staining was greatest at day 1 of pregnancy and gradually diminished, first in endothelial and then in epithelial cells, until there is little or no detection on day 5 (Fig.2B, A'–E').

On day 5 of pregnancy, luminal epithelial cells and stromal cells surrounding the embryo implantation site pooled pericellular peroxidasin in abundance compared to collagen IV (Fig.2B, E', E"). This striking up-regulation of peroxidasin was not observed in other surrounding tissues, such as the myometrium were comparative abundance of collagen IV and peroxidasin remained relatively similar to previous days of pregnancy (Fig.4 in [43]). In decidual tissues of days 6 through 8, peroxidasin remained localized to newly synthesized collagen IV (Fig.2B, F'–H'). By day 7 and 8 of pregnancy, some cytoplasmic peroxidasin was detected in addition to BM-associated peroxidasin (Fig.2B, G'–H'). Interestingly, the cells that were devoid of collagen IV around the day 8 embryo were positive for cytoplasmic peroxidasin (Fig.2B, H').

The up-regulation of peroxidasin by blastocysts attachment poses the question of whether this natural decidual reaction could also be induced by an experimentally controlled procedure. Progressions towards the development of embryo-induced decidua and oil-induced deciduomata generally have remarkably similar timing, expression profiles, and histology [58,59]. In the present study, day 6 deciduomata and deciduum displayed similar patterns of peroxidasin and collagen IV (Fig.2B, I' and F'). Together, these results demonstrated strong temporal and spatial expression and localization patterns of peroxidasin during the periimplantation period and which preceded expression of collagen IV, and persistent localization as decidua BM assembled around cells.

Peroxidasin catalyzes the formation of sulfilimine crosslinks between adjoining protomers of collagen IV, a structural reinforcement that is essential for tissue function [26–28]. We, therefore, sought to determine whether these crosslinks form during the switch from epithelial BM of the endometrium to mesenchymal-derived BM of the decidua. Endometrial and decidual explants were subjected to collagenase digestion to excise crosslinked NC1 domains of collagen IV, followed by immunoblot assays to assess the degree of crosslinking. We observed 37 kDa protein bands that correspond to single (D1) and double (D2) crosslinked NC1 domains, as previously described [26], along with less intense bands around 23 kDa that correspond to non-crosslinked NC1 monomeric domains. This crosslinking pattern was common for all samples (Fig.2C). Together, this study demonstrated that peroxidasin expression increased during periimplantation, localized to areas where new collagen IV was synthesized and crosslinked collagen IV across all stages of decidua development.

2.3. Goodpasture antigen-binding protein (GPBP) encoding gene expression and protein localization during early pregnancy

Expression of the GPBP encoding gene (*Col4a3bp*) gives rise to multiple isoforms, GPBP-1 and GPBP-2 (previously called GPBP and GPBPΔ26). One isoform, GPBP-1, preferentially localizes extracellular matrix. The alternatively spliced isoform, GPBP-2 also known as CERT, is predominately cytosolic where it functions in intraorganelle lipid transport and vesicular transport to the plasma membrane [33,34,60]. First, to determine whether any GPBP was expressed, we quantified mRNA expression levels during early pregnancy and decidua development. We found *Col4a3bp* expression followed bimodal temporal expression pattern during early pregnancy with the lowest expression during the periods of uterine receptivity and implantation, days 4 through 6 of pregnancy. After blastocyst implantation, *Col4a3bp* levels showed a gradual increase from days 5 through 8 of pregnancy (Fig.3A). These findings suggested that expression of *Col4a3bp* is reduced during the initiation of blastocyst implantation.

Next, we sought to examine the localization of GPBP protein by immunofluorescence using mAB N26 that detects of both GPBP-1 and GPBP-2 isoforms. On day 1 of pregnancy, GPBP was intensely localized in luminal and glandular epithelial cells with little or no localization detected in the stroma. The protein was predominantly localized to apical and basal plasma membrane of epithelial cells and showed diffuse cytoplasmic localization. Over the next few days (days 2 through 4), intracellular GPBP in the stroma and glands was decreased. However, a specific pattern of cellular localization was observed in the luminal epithelial cells at this time (Fig.3B, A'–D') (See also Fig.5 in [43]). By day 2 of pregnancy, membranous localization was receding and was being replaced by dense puncta oriented to the basal regions of the cells. Further changes were observed on day 3 of pregnancy with localization of GPBP to the lateral and apical regions of epithelial cells (Fig.3B, B'–C'). On days 4 and 5 of pregnancy, GPBP was primarily localized to the apical membrane of luminal epithelial cells, with little stromal localization (Fig.3B, D'–E').

As the decidualization processes progressed, the decidual zone surrounding the embryo showed strong GPBP localization from days 6 through 8 of pregnancy. Localization of GPBP on these days was observed at the cell borders and within the cytoplasm of decidual cells (Fig.3B, F'–H'). This increased localization temporally coincided with BM thickening (Fig.1C–D) and increased GPBP mRNA expression (Fig.3A). By day 8 of pregnancy, layers of decidual cells juxtaposed to the embryo were devoid of significant levels of GPBP localization, suggesting that GPBP was primarily expressed by decidual cells encapsulated by collagen IV (Fig.3B, H'). Accumulation of GPBP in the artificially-induced deciduomata displayed similar production by decidual cells as decidualization induced by the implanted blastocyst (Fig.3B I'). Collectively, the data revealed that expression and localization of both isoforms, GPBP-1 and GPBP-2, are down-regulated during uterine receptivity. However, it was unclear if one or both isoforms were amplified during decidualization, a feature that coincides with decidua BM thickening.

2.4. Localization patterns of GPBP-1 and laminin in the uterus during early pregnancy

Previous studies have revealed the GPBP-1 is associated with the extracellular matrix of kidney [REF]. We sought to determine if our findings of pericellular GPBP (Fig.3B) were associated with GPBP-1 translation and localization to basement membrane in the uterus. We used a novel monoclonal antibody (mAb e11-2) that recognizes the 26-residue region present in GPBP-1 but not in GPBP-2 (Fig.4A). We focused on days 1 through 3 and days 6 through 8 since higher levels of expression and detection of GPBP were observed during this time frame. The detection of GPBP-1 showed similar localization patterns as detection of one or both GPBP isoforms (Fig.4B and Fig.3B). GPBP-1 was primarily localized to epithelium day 1 through 3 and decidual zones days 6 through 8. Cytoplasmic puncta were observed on day 2 followed by apical localization on day 3 (Fig.4B, A'–C'). At that time, basal GPBP-1 was co-localized with laminin, a biomarker of BM, patterns concentrated to the upper most side of the basement membrane but not intensely throughout (Fig.4B, A"-C"). Laminin and GPBP were co-localized in myometrium and perimetrium throughout all pre- and postimplantation days of pregnancy (Fig.6 in [43]). Pericellular GPBP-1 co-localized with laminin in the decidual zone days 6 through 8, with days 7 and 8 showing the strongest detection of GPBP-1 (Fig.4B, D'–F'). Interestingly, different sides of individual cells had comparatively unequal distribution of GPBP-1 and laminin, according to relative intensities of co-localized regions (Fig.4, D"-F"). These decidual tissues had no presence of collagen IV alpha 3 (data not shown). Thus, the uterine BM-associated patterns of GPBP-1 were achieved through interactions with other BM components, such as previously described bindings with other chains of collagen IV and laminin [35]. Our findings of GPBP-1 immunofluorescence show that it 1) is the predominant isoform of GPBP in the uterus during early pregnancy, 2) localizes to endometrial and decidual BMs, and 3) has varied distribution around individual decidual cells.

2.5. Collagen IV and laminin gene expression and protein localization patterns in the uterus during early pregnancy

Thus far, many concepts that indicate BMs undergo dynamic regulation are based on studies in non-vertebrate animal models and cell culture systems [23–25]. In the present study, we examined uterine tissues as our model system because BM toolkit proteins, collagen IV and laminin, have been shown to localize in BMs in the endometrium before implantation and in mature decidua several days after implantation [12–15]. These pre- and postimplantation BMs associate with different tissues that occupy an overlapping anatomical space through tissue reprogramming, yet differ in fine details (Fig.1). However, the dynamic transition of these components upon embryo implantation and initial triggering of decidualization is unknown. We, therefore, sought to analyze mRNA expression levels of collagen IV (collagen IVα1 and collagen IVα2) and laminin (laminin γ1) by qPCR in the uterus throughout uterine reprogramming. The expression levels of *Col4a1*, *Col4a2* and *Lamc1* remained relatively constant from days 1 through 4 (Fig.5A). However, *Col4a2* levels showed significant up-regulation over *Lamc1* in day 5 implantation sites compared with their preimplantation uterine levels (days 1 through 4). While the levels of both genes for collagen IV chains showed no significant differences from days 5 through 8, *Lamc1* levels showed a steady increasing trend from days 5 through 8 (Fig.5A). These findings are consistent with a previous study that demonstrated the relative expressions of genes

encoding collagen IV and laminin in mouse uterus during early pregnancy using Northern and slot blot analysis [13]. Despite these compelling findings, definitive differences in protein localization of collagen IV and laminin have not been demonstrated, particularly during the period when expression seems to diverge with the incident of blastocyst attachment and early decidualization. We, therefore, applied co-immunofluorescences to examine the compartmental distribution associated with the differential expression of collagen IV and laminin proteins.

During the preimplantation period (days 1 through 4), collagen IV and laminin were co-localized exclusively beneath the BM of cells of the luminal epithelium, glandular epithelium and blood vessels in the endometrium. As expected, no collagen IV or laminin localization was detected in stromal cells at this time (Fig.5B, A'–D'). Following blastocyst attachment, collagen IV and laminin production were co-localized underneath the luminal epithelium and glandular epithelium in day 5 implantation sites. Notably, the implanted blastocyst was positive for laminin, but not for collagen IV. Additionally, we noticed for the first time weak detection of collagen IV and laminin throughout the stromal area (Fig.5B, E'). Interestingly, higher magnification images of the area beneath the attached blastocyst revealed punctate collagen IV deposition in the absence of laminin around decidual cells situated adjacent to the luminal epithelium (Fig.5B, E").

In the day 6 implantation site, punctate collagen IV staining surrounding decidual cells was observed with broader distribution into the growing decidual zone with limited detectable laminin. However, some peripheral stromal cells appeared to be positive for laminin (Fig.5B, F') (See also Fig.7 in [43]). These observations demonstrated that collagen IV preceded laminin expression and production in early differentiating stromal cells. On day 7 of pregnancy, laminin was co-localized with pericellular collagen IV puncta and the BM appeared to assemble into improved compact borders surrounding decidual cells (Fig.5B, G'). By day 8, collagen IV and laminin were co-localized and encapsulated individual decidual cells and distributed throughout the entire stromal space from near the embryo toward the myometrium (Fig.5B H')(See also Fig.7 in [43]). Interestingly, at this time, a few layers of cells juxtaposed to the embryo were consistently devoid of collagen IV and laminin staining. In the myometrium, collagen IV and laminin co-localized staining was observed as intense positive immunofluorescence around the muscle cells (Fig.7 in [43]). We observed the similar positive production of collagen IV and laminin in deciduomata tissue (Fig.5B, I'). Our results suggest that collagen IV deposition within pericellular spaces of the transitioning decidual zone may aid in the distinction of early decidual cells from stromal cells.

3. Discussion

Our findings of distinct spatial and temporal localization and expression patterns of peroxidasin, GPBP, collagen IV, and laminin within the reprogramming uterine tissues during early pregnancy suggest that these molecules are important players in the dynamic reorganization and functional changes that occur during decidua development. Our findings indicate that these ECM proteins possess both individual and integrated properties as

components of BM scaffolds. Moreover, our findings provide further evidence for the classification of peroxidasin and GPBP as components of the BM toolkit.

3.1. A potential dual function for peroxidasin in early pregnancy

We observed two novel distribution patterns of peroxidasin in association with the developing decidua. Peroxidasin was produced prior to collagen IV and then focused around stromal cells in their BM following embryo attachment, presumably, to confer continual sulfilimine crosslinking of collagen IV as it was deposited. We observed several instances of peroxidasin localized to tissue regions absent of BM. These findings suggest that in pregnancy peroxidasin may have physiological functions beyond its role in BM reinforcement. For example, peroxidasin generates intermediate products that have the potential to protect from infection at highly vulnerable stages in pregnancy. Low concentrations of hypohalous acids (HOBr and HOCl) produced by peroxidasin have been shown to have antimicrobial functions. Exposure of *E. coli* cultures to purified peroxidasin in the presence of its enzymatic substrates, H_2O_2 and chloride, results in the destruction of the bacteria [61]. Possibly, these antimicrobial mechanisms of peroxidasin may contribute to natural defense against microbial infections at the time of implantation and during early embryo development, thus protecting against the potential for pregnancy failure [62]. Notably, several microbes that disrupt decidua function, including the human papillomavirus (HPV) and *Staph. aureus*, have derived mechanisms that may dock microbes to or destroy BMs [63], further emphasizing the benefits of localization of an antimicrobial producing agent, such as peroxidasin, to decidual BMs. This is of particular interest when considering the milieu of the embryonic environment where the cells typically responsible for eliminating pathogens, such as dendritic cells and macrophages, have restricted mobility and functionality in the decidua [64–68].

3.2. Expression and Localization of GPBP potentially regulate BM thickening during decidualization

We found decidual GPBP was expressed after collagen IV and laminin are deposited. Interestingly, it was up-regulated as decidua BM was forming which suggests it may act as a key component in the assembly of new basement membranes in these adult tissues. We found the distribution of GPBP in BMs to vary in small domains around decidual cells that coincide with a variably progressive thickening of BM ultrastructure around these cells. Similarly, overexpression of GPBP has been previously shown to induce renal BM thickening in a mouse model [36]. Micro-tailored BM regions have essential physiological functions customized to modulating behaviors of cells in elegant systems such as synaptic BMs that differ from extrasynaptic BMs at neuromuscular junctions [6] and BM pliability that orchestrates transmigration of individual cells during development [22]. Thus, BM thickening and GPBP expression may be important contributors of the normal function of the decidua.

A previous study showed that early decidua tissue (approximately day 6 of pregnancy) has a quantitative tensile strength of averaging 23 kPa which is sufficient enough to exert forces on the embryo for elongation and formation of the distal visceral endoderm [69]. This tensile strength is comparable to soft tissues, such as striated and myocardial smooth muscles,

which are almost entirely comprised of specialized cells encapsulated in BM [70]. Such tissues are designed to endure and respond to the greatest natural forces challenging the corpus. We presume mature decidual tissue (day 8 of pregnancy) has even greater tensile strength than the reported day 6 decidual tissues because of our findings of an even thicker BM. This notion is further supported by previous findings that associate progressive thickening of embryonic retinal BM with a substantial increase in tensile strength [71].

3.3 Basement membrane in preimplantation uterus

Our findings of collagen IV and laminin co-localization underlying polarized epithelial cells of the lumen and glands, and endothelial cells of blood vessels in the preimplantation mouse uterus, is an expected observation since these proteins are the most abundant BM components and classically co-localize in BMs throughout the body [1]. However, a significant finding of the present study was the unique expression and localization patterns of peroxidasin and GPBP in uterine epithelial cells prior to implantation. GPBP is a protein with multiple isoforms that function both at extracellular and intracellular compartments [72]. Both intracellular and pericellular localization of this protein in days 1 and 2 of pregnancy suggests it may serve in dual roles in intraorganelle protein transport for plasma membrane transformation [73] and/or in the molecular organization of BM components [36], respectively.

We also found peroxidasin to have intracellular localization and pericellular co-localization with collagen IV in the preimplantation uterine epithelial cells, which suggests active turnover and application of the enzyme in BM reinforcement by sulfilimine crosslinking. Peroxidasin is a specific peroxidase critical for the maintenance of epithelial tissue integrity across several species and organ systems [27]. Perturbation of its function yields epithelium disorganized and dysfunctional [26,29,74]. Therefore, it is likely that peroxidasin reinforces the collagen IV network of BM scaffolds to support epithelial cell architecture in the endometrium. In the endometrium, BM interfaces the epithelium and the stroma thus mediating communication between these compartments by its known functions of engaging cell-matrix signaling and modulating chemokine signaling forming cytokine gradients and acting as growth factor reservoirs [75]. The importance of the communication between these tissue compartments is represented in the mouse models that show a failure of blastocyst implantation or decidualization in the absence of endometrial glands [76] or luminal epithelium [77]. In this regard, the presence of BM within the preimplantation endometrium has importance in governing for uterine receptivity, blastocyst implantation, and decidualization.

3.4. Collective functions of BM components during decidualization

In response to blastocyst implantation, we observed collagen IV is distinctively associated with stromal cells surrounding the implanted blastocyst independent of laminin localization indicating that collagen IV may be important for early alterations of these cells. Current dogma argues that laminin is the pivotal BM component produced by cells forming new BMs [78,79]. However, most studies contributing to this perception focus on embryo development and do not address BM production in adult tissues. Our observations herein

suggest that the order of collagen IV and laminin expression may be tissue and context specific.

One of the hallmarks of decidualization is the proliferation of stromal cells prior to the transition to decidual cells [41]. Studies have demonstrated that collagen IV and laminin are required for cell proliferation and/or differentiation in epithelial, endothelial, and some mesenchymal cells such as muscle cells [1–3,7]. Our results suggest that decidual cells are perhaps another cell type reliant on these BM properties. Epithelial-mesenchymal transition (EMT) is considered to be a fundamental event during embryogenesis, while a reverse cell fate (mesenchymal-epithelial transition, MET) was also described during cellular reprogramming [80]. Following blastocyst implantation, stromal cells surrounding the implanted blastocyst undergo polyclonal decidualization which is crucial to sustaining pregnancy since epithelial cells surrounding the blastocyst disappear by apoptosis [41]. Several studies have provided evidence that decidual cells are perhaps epithelial-like cells since stromal cells loose mesenchymal makers proteins like snail and vimentin [81] and gain epithelial marker proteins like E-cadherin, zonula occludens-1 (ZO-1) and cytokeratin [82] during stromal to decidual transition. Consistent with these findings, we report mesenchymal-derived decidual cells formed basement membrane in their pericellular spaces with up-regulated peroxidasin, GPBP, collagen IV, and laminin. The BM produced by decidual cells provides an additional evidence of epithelial-like behavior which supports the concept that MET is a normal process during pregnancy. In addition to representing a hallmark of epithelial-like differentiation, the interplay of cell-matrix interactions and inclusion of BM-bound chemokines and growth factors, such as bone morphogenic proteins (BMPs) [44,83], transforming growth factor-beta (TGFβ), heparin-binding epidermal growth factor-like growth factor (HB-EGF), and fibroblast growth factor 10 (FGF10) [75,84,85], may modulate endometrial stromal cell proliferation and MET.

We also found BM to encapsulate stromal cells early in decidualization but noted continuity of BM structure was altered with the appearance of cell-cell junctions as decidual cells matured. It is known that cell-cell junctions are features of decidua establishment and function as macromolecular barriers between the mother and embryo which can block penetrance of IgG that can elicit unwanted immune rejection of the embryo and add rigidity to the tissue [86,87]. Interestingly, a recent study on cardiomyocytes, a mesenchymal-derived cell encapsulated by BM, showed a similar pericellular BM that underwent alterations for the mediation of cell junction formation [88]. Perhaps decidua BM also mediates tight junction formation and functions as an additional selective barrier and contributes to rigidly while junctions are established.

3.5. Pregnancy and pseudo-pregnancy BM production response convergence

We found that embryo-induced and oil-induced decidualization produced similar distributions of BM toolkit proteins peroxidasin, GPBP, collagen IV, and laminin within similar timeframes (Figs.2B, 3B, and 5B). Thus, our findings demonstrate commonalities in the mechanisms of uterine reprogramming that are triggered by natural embryonic implantation and pseudo-pregnancy. Further studies that compare responses to these stimuli will give insights into the mechanisms whereby the embryo triggers BM changes.

3.6. Conclusion

In summary, we show that peroxidasin, GPBP, collagen IV, and laminin are expressed in temporal and spatial patterns during uterus reprogramming, suggesting individual functions of these ECM components and collective functions as components of BMs (Fig.6). Such matrix modulation is congruous with the emerging concept that BMs are more than static scaffolds whereby they influence cell fate, behavior, and tissue stability and function [23,24]. The underlining cell-BM interactions may be disrupted in spontaneous abortion [89], diabetes [18,90], nutrition [28], and smoking [91]. Importantly, our findings provide evidence that peroxidasin and GPBP are critical ECM components for embryo implantation and decidua development and supportive evidence for their classification as components of the BM toolkit. Furthermore, mouse embryo implantation can serve as a tractable model for the exploration of the functions of BM toolkit of proteins during early pregnancy and in many aspects of human uterine physiology [12,44,45,92].

4. Experimental Procedures

4.1. Animals

Sexually mature CD1 mice were used for all studies (Charles River Laboratories, Crl:CD1(ICR), Wilmington, MA, USA). Female mice were bred overnight with fertile males of the same strain and the presence of vaginal plug the following morning indicated day 1 of pregnancy [41]. On days 1 through 4 of pregnancy, whole uterine horns were harvested. Implantation sites on day 5 of pregnancy were identified after intravenous injections of 1% Chicago Blue 6B dye (Sigma, St. Louis, MO) in saline (0.1 mL/mouse) [93]. On days 6 through 8 of pregnancy, implantation sites were collected by visual identification. All samples were collected on the morning of the determined day of pregnancy between 0830–0930 hours, snap frozen in Freeze'It (Fisher Scientific, Waltham, MA), and stored at −80°C until further processing. To induce artificial decidualization, referred to as deciduomata, the uterine horn was injected intraluminally with 20 μl of sesame oil on the morning of day 4 of pregnancy eliciting a hormonally primed inflammatory decidual reaction without embryo attachment [58,59]. Embryos were expelled from the uterine horn or do not survive the oil injection [94]. Artificially-induced decidual tissues were collected for immunofluorescence studies 48 hours post injection on day 6. All animal procedures were conducted in accordance with guidelines and standards of the Society for the Study of Reproduction (SSR) and approved by Vanderbilt University's Institutional Animal Care and Use Committee (IACUC).

4.2. Transmission Electron Microscopy (TEM)

Fresh uterine tissues were immediately fixed in 5 mL of 2.5% glutaraldehyde solution in 0.1 M sodium cacodylate buffer (w/v) for 2 hours at room temperature followed by an additional 24 hours at 4°C and were transported to Vanderbilt's Cell Imaging Shared Resource for further processing. Tissues were rinsed with 0.1 M cacodylate buffer, fixed in 1% osmium tetraoxide for 1 hour and rinsed again with 0.1 M cacodylate buffer at room temperature. Subsequently, the samples were dehydrated in ascending grades of ethanol and passed through 2 exchanges of pure propylene oxide (PO). Samples were next infiltrated with several exchanges of resin and PO as follows: 25% Epon 812 epoxy resin (ER): 75%PO

(v/v), 50%ER: 50%PO twice, 75%ER: 25%PO, and 100% ER twice. The samples were incubated several hours with fresh 100% ER and then placed at 60°C for 48 hours for polymerization [28]. Ultra-thin sections (70–80 nm) were cut from the regions of interest using an ultramicrotome (Leica ultracut, Buffalo Grove, IL) and mounted on 300-mesh copper grids. The sections were stained at room temperature with 2% uranyl acetate (w/v) for 15 minutes followed by Reynold lead citrate for 10 minutes.

Two ultra-thin sections per group were examined in a Philips T-12 electron microscope (FEI, Hillsboro, OR), and 11,000x- 30,000x micrographs were collected with AMT CCD and Gatan CCD camera systems. Particular attention was given to basement membrane material identified as lamina densa in pericellular space, adjacent to cells, with some clear linearity. Basement membranes were marked by 100nm dots using paint tool in Photoshop (CS6, Adobe). These measurements were arrayed along the lamina densa orthogonally to relative regional x-axes at 100 nm intervals (between dot markers) using line measurement function in FIJI (1.49q, ImageJ). Membrane thickness was quantified across 11 to 15 fields of view at 11,000x or 15,000x and pooled by groups for analysis of 1,300 measurements.

4.3. Quantitative real-time polymerase chain reaction (qPCR)

Total RNA from uterine tissues (whole uterine horns (days 1 through 4) and implantation sites (days 5 through 8) was prepared using guanidine isothiocyanate-phenol-chloroform extraction method [42]. Extraction was inclusive of all cell types. Other data has been included to assess the compartmental localization of proteins that result from translation of the expressed mRNA. DNase-treated (Bio-Rad, Hercules, CA) RNA (2.5 μg) was reverse transcript using SuperScript III and the included oligo(dT) primers per manufacturer's instructions (Life Technologies, Grand Island, NY). The cDNA (1 μL) was amplified in 20 μl total volume using iQ SYBER Green Supermix (Bio-rad, Hercules, CA) and specific primers for *Col4a1* (collagen IV, α1 encoding gene), *Col4a2* (collagen IV, α2 encoding gene), *Lamc1* (laminin γ1 subunit encoding gene), *Pxdn* (peroxidasin encoding gene), *Col4a3bp* (all isoforms of GPBP encoding gene), and *Rpl7* (ribosomal protein L7 encoding gene) (Table 1). The following qPCR protocol was used: 95°C for 3 min followed by 40 cycles of 95°C for 10 seconds and 60°C for 30 seconds. All reactions were run in triplicates. Data was collected on a CFX96 system with CFX Manager software (version 3.1, Bio-rad, Hercules, CA) and was analyzed by 2^(−delta delta Ct) method for fold change. Data was normalized to *Rpl7*, a commonly used reference gene.

4.4 Immunofluorescence

Frozen tissues were warmed to −20°C, embedded in Optimal Cutting Temperature (OCT) compound (Sakura Tissue-Tek, Torrance, CA) and sectioned (12 μm) in a cryostat (Leica Biosystems, Buffalo Grove, IL). Sections were collected on Superfrost Plus slides (Fisher Scientific, Waltham, MA), air-dried and fixed in −20°C acetone for 10 minutes. Slides were washed several times with phosphate-buffered saline (PBS) (Corning, Corning, NY) and PBS/0.2% Tween (Sigma, St. Louis, MO). Slides to be stained with collagen IV antibody (JK2) were treated with dissociation buffer consisting of 6M urea in 0.1 M glycine buffer (pH 3.0) [95] followed by several washes with PBS and PBS/0.2% Tween. Laminin and peroxidasin immunodetection patterns were minimally influenced by dissociation treatment

rendering co-immunostaining with collagen IV antibody possible [43]. Immunodetection of GPBP and co-localization with laminin was achieved without the dissociation step because GPBP antibodies used in this study failed to show specific staining in sections treated with the dissociation buffer. All sections were preincubated with 10% normal serum from goat or horse (Invitrogen, Grand Island, NY) for 1 hour at room temperature to avoid nonspecific binding of antibodies prior to applying primary antibodies. The following primary antibodies were used for antigen detections: rat anti-collagen IV NC1 (1:500 dilution, JK2, were from Y. Sado, Shigei Medical Research Institute, Okayama, Japan [95,96]), rabbit anti-laminin (1:50 dilution for tissues not treated with dissociation buffer and 1:500 dilution for those that were pre-treated with dissociation buffer, ab11575, Abcam, Cambridge, MA), rabbit anti-peroxidasin (1:250 dilution, were from G. Bhave, Vanderbilt University, Nashville, TN [27]), Alexa546 conjugated mouse anti-GPBP (1:50 dilution, mAb N26 to the N-terminal serine-rich domain conserved across all GPBP isoforms in several species [97], from Fibrostatin, SL, Valencia, Spain), and Alexa546 conjugated mouse anti-GPBP-1 (1:50 dilution, mAb e11-2 to the 26-amino acid residue of exon 11 not present in GPBP-2, also called CERT [60], from FIbrostatin, SL, Valencia, Spain). The secondary antibodies used for immunofluorescence detection were: Alexa555 goat anti-rat (1:200 dilution, ab150166, Abcam) and Alexa488 goat anti-rabbit (1:200 dilution, ab150081, Abcam). All primary antibodies were diluted in PBS/0.1% Tween and 5% normal goat serum. Sections were incubated with these antibodies overnight at 4°C in a humidified chamber and then washed three times with PBS/0.2% Tween. Negative control samples were processed similarly to experimental samples but without the inclusion of primary antibodies. Diluted secondary antibodies were applied to sections for 1 hour at room temperature. After several washes, 1 μM Hoechst fluorescent dye was applied (10 minutes) for labeling cell nuclei. Following washes in PBS/0.2% tween and PBS, sections were mounted in Prolong Gold (Life Technologies, Grand Island, NY) and cured at room temperature for 2 days. Images at 0.323 μm/pixel resolutions were captured utilizing the Ariol SL-50 or Apiro Versa 200 automated fluorescent microscopes with a 20x objective (Leica Biosystems, Buffalo Grove, IL) housed in the Vanderbilt Digital Histology Shared Resource. Image linear brightness and contrast were adjusted for visual comparison using FIJI (1.49q, ImageJ, NIH, Bethesda, **Maryland**) controlling for within set staining and to maintain consistent intensities relative to representative controls (see Fig.4–7 in [43]).

4.5. Isolation of Collagen IV NC1 Hexamers

Uterine endometrial tissues from days 4 through 8 were separated from the myometrium casing by firm rolling pressure along the uterine horn. Both endometrial and myometrium samples were snap frozen in Freeze'It (Fisher Scientific; Waltham, MA). Frozen samples were added to preweighed 1.5 mL microcentrifuge tubes containing 100 μL of isolation buffer [50 mM Hepes (pH 7.5), 10 mM CaCl2, 1 mM PMSF, 5 mM benzamadine-HCl, 25 mM 6-amino-n-hexanoic acid]. A micropestle was used to disperse each sample; residual tissue was washed from the micropestle with 200 μL of isolation buffer and added to the sample. The suspension was homogenized by sonication in an ice water bath for approximately 5 minutes followed by centrifugation at 10,000 × g for 15 minutes. The soluble fraction was discarded and the mass of the remaining insoluble material was measured and recorded. Two milliliters of isolation buffer containing 0.1 mg mL^{-1} bacterial

collagenase (Worthington Biochemical; Lakewood, NJ) was added to the samples per gram of pellet obtained. The sample was briefly mixed by vortex and subjected to sonication to loosen the pellet. Samples were allowed to digest at 37°C with shaking for 24 hours. The solubilized NC1 fraction was collected in the supernatant after centrifugation at 14,000x g for 30 minutes. The isolated fraction was used for immunoblot analysis [26].

4.6. Immunoblot

Collagen IV NC1 hexamers were analyzed by SDS/PAGE in 12% (wt/vol) *bis*-acrylamide mini-gels with Tris-Glycine-SDS running buffer. Ten microliters of each sample were loaded using 4x LDS sample buffer (Bio-rad, Hercules, CA). Each sample was derived from individual mice and the loading order was consistent between endometrium and myometrium. After electrophoresis under non-reducing conditions, proteins were transferred to 0.2μm pore sized PVDF membrane (Bio-rad, Hercules, CA) [26]. Immunodetection was carried out per manufacturer recommendations (LI-COR, Doc #988-13627, Lincoln, NE). Immunoreactivity and detection were achieved with primary antibody JK2 (1:2500) and secondary antibody goat anti-rat IRDye 680LT (1:20,000; LI-COR 926–68029, Lincoln, NE). Immunoreactivity was quantified by near-infrared signals detected using Odyssey Classic (LI-COR, Lincoln, NE, provided by Vanderbilt University Initiative for Maximizing Student Diversity shared equipment) and signals were analyzed using Image Studio Lite (LI-COR, Lincoln, NE).

4.7. Statistics

Statistical analysis and graphing was performed using SPSS Statistics (Version 22, IBM). For qPCR data analysis, independent variables two-tailed T-test was used with equal variance not assumed. For TEM data analysis, non-parametric independent-samples tests, Kruskal-Wallis and Median tests, were performed along with posthoc pairwise comparisons of distributions. The significance level was set at p-value ≤ 0.05.

Supplementary Material

Refer to Web version on PubMed Central for supplementary material.

Acknowledgments

We acknowledge the invaluable editorial efforts of Kathleen Dennis, Ph.D. at Vanderbilt University Medical Center; the admirable efforts of Wei Lei, Ph.D. and Sergei Chetyrkin, Ph.D. for designing and screening of primers while working with the Aspirnaut interns at Vanderbilt University Medical Center, including Arnez Orr; and the valuable efforts of Fernando Revert, Ph.D. for producing and characterizing novel antibodies (mAb N26 and mAb e11-2) at Fibrostatin, SL. This work was supported by the National Institutes of Health [grants F31 CA165787-03 (to C.R.J.), R25 DK096999 (to B.G.H. for S.P. and T.B.), K08 DK097306 (to G.B.), R01 HD044741 (to B.C.P.), and R01 DK018381 (to B.G.H)]. This study was also supported by RT2014-2415-1 / Prometeo II −2014-048 (to J.S).

Abbreviations

BM(s)	Basement membrane(s)
ECM	extracellular matrix
GPBP	Goodpasture antigen-binding protein

References

1. Yurchenco PD. Basement membranes: Cell scaffoldings and signaling platforms. Cold Spring Harb. Perspect. Biol. 2011; 3:1–27.
2. Hynes RO. The extracellular matrix: not just pretty fibrils. Science. 2009; 326:1216–1219. [PubMed: 19965464]
3. Hagios C, Lochter A, Bissell MJ. Tissue architecture: the ultimate regulator of epithelial function? Philos. Trans. R. Soc. Lond. B. Biol. Sci. 1998; 353:857–870. [PubMed: 9684283]
4. Davis GE, Senger DR. Endothelial extracellular matrix: biosynthesis, remodeling, and functions during vascular morphogenesis and neovessel stabilization. Circ. Res. 2005; 97:1093–1107. [PubMed: 16306453]
5. Campbell KP, Stull JT. Skeletal muscle basement membrane-sarcolemma-cytoskeleton interaction minireview series. J. Biol. Chem. 2003; 278:12599–12600. [PubMed: 12556456]
6. Sanes JR. The basement membrane/basal lamina of skeletal muscle. J. Biol. Chem. 2003; 278:12601–12604. [PubMed: 12556454]
7. Boonen KJM, Post MJ. The muscle stem cell niche: regulation of satellite cells during regeneration. Tissue Eng. Part B. Rev. 2008; 14:419–431. [PubMed: 18817477]
8. Sillat T, Saat R, Pöllänen R, Hukkanen M, Takagi M, Konttinen YT. Basement membrane collagen type IV expression by human mesenchymal stem cells during adipogenic differentiation. J. Cell. Mol. Med. 2012; 16:1485–1495. [PubMed: 21883898]
9. Kubo Y, Kaidzu S, Nakajima I, Takenouchi K, Nakamura F. Organization of extracellular matrix components during differentiation of adipocytes in long-term culture. In Vitro Cell. Dev. Biol. Anim. 2000; 36:38–44. [PubMed: 10691039]
10. Court FA, Wrabetz L, Feltri ML. Basal lamina: Schwann cells wrap to the rhythm of space-time. Curr. Opin. Neurobiol. 2006; 16:501–507. [PubMed: 16956757]
11. Scherer SS. The biology and pathobiology of Schwann cells. Curr. Opin. Neurol. 1997; 10:386–397. [PubMed: 9330884]
12. Wewer UM, Faber M, Liotta LA, Albrechtsen R. Immunochemical and ultrastructural assessment of the nature of the pericellular basement membrane of human decidual cells. Lab. Invest. 1985; 53:624–633. [PubMed: 2415774]
13. Farrar JD, Carson DD. Differential temporal and spatial expression of mRNA encoding extracellular matrix components in decidua during the peri-implantation period. Biol. Reprod. 1992; 46:1095–1108. [PubMed: 1391307]
14. Oefner CM, Sharkey A, Gardner L, Critchley H, Oyen M, Moffett A. Collagen type IV at the fetal-maternal interface. Placenta. 2014
15. Diao H, Aplin JD, Xiao S, Chun J, Li Z, Chen S, et al. Altered Spatiotemporal Expression of Collagen Types I, III, IV, and VI in Lpar3-Deficient Peri-Implantation Mouse Uterus. Biol. Reprod. 2011; 84:255–265. [PubMed: 20864640]
16. Lukashev ME, Werb Z. ECM signalling: Orchestrating cell behaviour and misbehaviour. Trends Cell Biol. 1998; 8:437–441. [PubMed: 9854310]
17. Fang M, Yuan J, Peng C, Li Y. Collagen as a double-edged sword in tumor progression. Tumour Biol. 2014; 35:2871–2882. [PubMed: 24338768]
18. Yurchenco PD, Patton BL. Developmental and pathogenic mechanisms of basement membrane assembly. Curr. Pharm. Des. 2009; 15:1277–1294. [PubMed: 19355968]
19. Khoshnoodi J, Pedchenko V, Hudson BG. Mammalian collagen IV. Microsc. Res. Tech. 2008; 71:357–370. [PubMed: 18219669]
20. Pöschl E, Schlötzer-Schrehardt U, Brachvogel B, Saito K, Ninomiya Y, Mayer U. Collagen IV is essential for basement membrane stability but dispensable for initiation of its assembly during early development. Development. 2004; 131:1619–1628. [PubMed: 14998921]
21. Miner JH, Li C, Mudd JL, Go G, Sutherland AE. Compositional and structural requirements for laminin and basement membranes during mouse embryo implantation and gastrulation. Development. 2004; 131:2247–2256. [PubMed: 15102706]

22. Kelley LC, Lohmer LL, Hagedorn EJ, Sherwood DR. Traversing the basement membrane in vivo: a diversity of strategies. J. Cell Biol. 2014; 204:291–302. [PubMed: 24493586]
23. Isabella AJ, Horne-Badovinac S. Dynamic regulation of basement membrane protein levels promotes egg chamber elongation in Drosophila. Dev. Biol. 2015
24. Morrissey MA, Sherwood DR. An active role for basement membrane assembly and modification in tissue sculpting. J. Cell Sci. 2015; 128:1661–1668. [PubMed: 25717004]
25. Xu R, Boudreau A, Bissell MJ. Tissue architecture and function: dynamic reciprocity via extra- and intra-cellular matrices. Cancer Metastasis Rev. 2009; 28:167–176. [PubMed: 19160017]
26. Fidler AL, Vanacore RM, V Chetyrkin S, Pedchenko VK, Bhave G, Yin VP, et al. A unique covalent bond in basement membrane is a primordial innovation for tissue evolution. Proc. Natl. Acad. Sci. U. S. A. 2014; 111:331–336. [PubMed: 24344311]
27. Bhave G, Cummings CF, Vanacore RM, Kumagai-Cresse C, Ero-Tolliver IA, Rafi M, et al. Peroxidasin forms sulfilimine chemical bonds using hypohalous acids in tissue genesis. Nat. Chem. Biol. 2012; 8:784–790. [PubMed: 22842973]
28. McCall AS, Cummings CF, Bhave G, Vanacore R, Page-Mccaw A, Hudson BG. Bromine is an essential trace element for assembly of collagen IV scaffolds in tissue development and architecture. Cell. 2014; 157:1380–1392. [PubMed: 24906154]
29. Yan X, Sabrautzki S, Horsch M, Fuchs H, Gailus-Durner V, Beckers J, et al. Peroxidasin is essential for eye development in the mouse. Hum. Mol. Genet. 2014; 23:1–18. [PubMed: 23933734]
30. Khan K, Rudkin A, Parry DA, Burdon KP, McKibbin M, Logan CV, et al. Homozygous mutations in PXDN cause congenital cataract, corneal opacity, and developmental glaucoma. Am. J. Hum. Genet. 2011; 89:464–473. [PubMed: 21907015]
31. Gotenstein JR, Swale RE, Fukuda T, Wu Z, Giurumescu CA, Goncharov A, et al. The C. elegans peroxidasin PXN-2 is essential for embryonic morphogenesis and inhibits adult axon regeneration. Development. 2010; 137:3603–3613. [PubMed: 20876652]
32. Cummings CF, Pedchenko V, Brown KL, Colon S, Rafi M, Jones-Paris C, et al. Extracellular chloride signals collagen IV network assembly during basement membrane formation. J. Cell Biol. 2016; 213:479–494. [PubMed: 27216258]
33. Raya A, Revert F, Navarro S, Saus J. Characterization of a Novel Type of Serine / Threonine Kinase That Specifically Phosphorylates the Human Goodpasture Antigen. 1999; 274:12642–12649.
34. Revert F, Ventura I, Martínez-Martínez P, Granero-Moltó F, Revert-Ros F, Macías J, et al. Goodpasture antigen-binding protein is a soluble exportable protein that interacts with type IV collagen. Identification of novel membrane-bound isoforms. J. Biol. Chem. 2008; 283:30246–30255. [PubMed: 18772132]
35. Mencarelli C, Bode GH, Losen M, Kulharia M, Molenaar PC, Veerhuis R, et al. Goodpasture antigen-binding protein/ceramide transporter binds to human serum amyloid P-component and is present in brain amyloid plaques. J. Biol. Chem. 2012; 287:14897–14911. [PubMed: 22396542]
36. Revert F, Merino R, Monteagudo C, Macias J, Peydró A, Alcácer J, et al. Increased Goodpasture antigen-binding protein expression induces type IV collagen disorganization eposit of immunoglobulin A in glomerular basement membrane. Am. J. Pathol. 2007; 171:1419–1430. [PubMed: 17916599]
37. Raya A, Revert-Ros F, Martinez-Martinez P, Navarro S, Rosello E, Vieites B, et al. Goodpasture Antigen-binding Protein, the Kinase That Phosphorylates the Goodpasture Antigen, Is an Alternatively Spliced Variant Implicated in Autoimmune Pathogenesis. J. Biol. Chem. 2000; 275:40392–40399. [PubMed: 11007769]
38. Wagner GP, Kin K, Muglia L, Pavličev M. Evolution of mammalian pregnancy and the origin of the decidual stromal cell. Int. J. Dev. Biol. 2014; 58:117–126. [PubMed: 25023677]
39. Gellersen B, Brosens IA, Brosens JJ. Decidualization of the human endometrium: mechanisms, functions, and clinical perspectives. Semin. Reprod. Med. 2007; 25:445–453. [PubMed: 17960529]
40. Mester I, Martel D, Psychoyos A, Baulieu EE. Hormonal control of oestrogen receptor in uterus and receptivity for ovoimplantation in the rat. Nature. 1974; 250:776–778. [PubMed: 4370071]

41. Zhang Q, Paria BC. Importance of uterine cell death, renewal, and their hormonal regulation in hamsters that show progesterone-dependent implantation. Endocrinology. 2006; 147:2215–2227. [PubMed: 16469810]
42. Wang X, Matsumoto H, Zhao X, Das SK, Paria BC. Embryonic signals direct the formation of tight junctional permeability barrier in the decidualizing stroma during embryo implantation. J. Cell Sci. 2004; 117:53–62. [PubMed: 14627626]
43. Jones-Paris CR, Paria S, Berg T, Saus J, Bhave G, Paria BC, et al. Basement membrane ultrastructure and component localization data from early pregnancy mouse uterine tissues, Data in Br. submitted. 2016
44. Lim HJ, Wang H. Uterine disorders and pregnancy complications: insights from mouse models. J. Clin. Invest. 2010; 120:1004–1015. [PubMed: 20364098]
45. Ramathal CY, Bagchi IC, Taylor RN, Bagchi MK. Endometrial decidualization: of mice and men. Semin. Reprod. Med. 2010; 28:17–26. [PubMed: 20104425]
46. Rashid NA, Lalitkumar S, Lalitkumar PG, Gemzell-Danielsson K. Endometrial receptivity and human embryo implantation. Am. J. Reprod. Immunol. 2011; 66:23–30. [PubMed: 21726335]
47. Yoshinaga K. A sequence of events in the uterus prior to implantation in the mouse. J. Assist. Reprod. Genet. 2013; 30:1017–1022. [PubMed: 24052329]
48. Hantak AM, Bagchi IC, Bagchi MK. Role of uterine stromal-epithelial crosstalk in embryo implantation. Int. J. Dev. Biol. 2014; 58:139–146. [PubMed: 25023679]
49. Pawar S, Laws MJ, Bagchi IC, Bagchi MK. Uterine epithelial estrogen receptor alpha controls decidualization via a paracrine mechanism. Mol. Endocrinol. 2015; 29:me20151142.
50. Grant KS. Effect of Mouse Uterine Stromal Cells on Epithelial Cell Transepithelial Resistance (TER) and TNFalpha and TGFbeta Release in Culture. Biol. Reprod. 2003; 69:1091–1098. [PubMed: 12773432]
51. Paria BC, Song H, Dey SK. Implantation: Molecular basis of embryo-uterine dialogue. Int. J. Dev. Biol. 2001; 45:597–605. [PubMed: 11417904]
52. Dey SK, Lim H, Das SK, Reese J, Paria BC, Daikoku T, et al. Molecular Cues to Implantation. 2013
53. Sroga JM, Ma X, Das SK. Developmental regulation of decidual cell polyploidy at the site of implantation. Front. Biosci. (Schol. Ed). 2012; 4:1475–1486. [PubMed: 22652887]
54. Serman A, Serman L. Development of placenta in a rodent--model for human placentation. Front. Biosci. (Elite Ed). 2011; 3:233–239. [PubMed: 21196303]
55. Nelson CM, Bissell MJ. Of extracellular matrix, scaffolds, and signaling: tissue architecture regulates development, homeostasis, and cancer. Annu. Rev. Cell Dev. Biol. 2006; 22:287–309. [PubMed: 16824016]
56. Nelson RE, Fessler LI, Takagi Y, Blumberg B, Keene DR, Olson PF, et al. Peroxidasin: a novel enzyme-matrix protein of Drosophila development. EMBO J. 1994; 13:3438–3447. [PubMed: 8062820]
57. Paria BC, Tan J, Lubahn DB, Dey SK, Das SK. Uterine decidual response occurs in estrogen receptor-alpha-deficient mice. Endocrinology. 1999; 140:2704–2710.
58. Kennedy TG. Timing of uterine sensitivity for the decidual cell reaction: role of prostaglandins. Biol. Reprod. 1980; 22:519–525. [PubMed: 7388104]
59. Herington JL, Underwood T, McConaha M, Bany BM. Paracrine signals from the mouse conceptus are not required for the normal progression of decidualization. Endocrinology. 2009; 150:4404–4413. [PubMed: 19520782]
60. Revert-Ros F, López-Pascual E, Granero-Moltó F, Macías J, Breyer R, Zent R, et al. Goodpasture Antigen-binding Protein (GPBP) directs myofibril formation: Identification of intracellular downstream effector 130-kDa GPBP-interacting protein (GIP130). J. Biol. Chem. 2011; 286:35030–35043. [PubMed: 21832087]
61. Li H, Cao Z, Moore DR, Jackson PL, Barnes S, Lambeth JD, et al. Microbicidal activity of vascular peroxidase 1 in human plasma via generation of hypochlorous acid. Infect. Immun. 2012; 80:2528–2537. [PubMed: 22526679]
62. King AE, Kelly RW, Sallenave J-M, Bocking AD, Challis JRG. Innate immune defences in the human uterus during pregnancy. Placenta. 2007; 28:1099–1106. [PubMed: 17664005]

63. Steukers L, Glorieux S, Vandekerckhove AP, Favoreel HW, Nauwynck HJ. Diverse microbial interactions with the basement membrane barrier. Trends Microbiol. 2012; 20:147–155. [PubMed: 22300759]
64. Yoshinaga K. Two Concepts on the Immunological Aspect of Blastocyst Implantation. J. Reprod. Dev. 2012; 58:196–203. [PubMed: 22738903]
65. Collins MK, Tay C-SS, Erlebacher A. Dendritic cell entrapment within the pregnant uterus inhibits immune surveillance of the maternal/fetal interface in mice. J. Clin. Invest. 2009; 119:2062–2073. [PubMed: 19546507]
66. Chakraborty R, Pulendran B. Restraining order for dendritic cells: all quiet on the fetal front. J. Clin. Invest. 2009; 119:1854–1857. [PubMed: 19603541]
67. Hsu P, Nanan RKH. Innate and adaptive immune interactions at the fetal-maternal interface in healthy human pregnancy and pre-eclampsia. Front. Immunol. 2014; 5:125. [PubMed: 24734032]
68. Burrows TD, King A, Loke YW. The role of integrins in adhesion of decidual NK cells to extracellular matrix and decidual stromal cells. Cell. Immunol. 1995; 166:53–61. [PubMed: 7585981]
69. Hiramatsu R, Matsuoka T, Kimura-Yoshida C, Han S-W, Mochida K, Adachi T, et al. External mechanical cues trigger the establishment of the anterior-posterior axis in early mouse embryos. Dev. Cell. 2013; 27:131–144. [PubMed: 24176640]
70. Butcher DT, Alliston T, Weaver VM. A tense situation: forcing tumour progression. Nat. Rev. Cancer. 2009; 9:108–122. [PubMed: 19165226]
71. Candiello J, Balasubramani M, Schreiber EM, Cole GJ, Mayer U, Halfter W, et al. Biomechanical properties of native basement membranes. FEBS J. 2007; 274:2897–2908. [PubMed: 17488283]
72. Mencarelli C, Losen M, Hammels C, De Vry J, Hesselink MKC, Steinbusch HWM, et al. The ceramide transporter and the Goodpasture antigen binding protein: one protein--one function? J. Neurochem. 2010; 113:1369–1386. [PubMed: 20236389]
73. Murphy CR. Uterine receptivity and the plasma membrane transformation. Cell Res. 2004; 14:259–267. [PubMed: 15353123]
74. McCall AS, Cummings CF, Bhave G, Vanacore R, Page-McCaw A, Hudson BG. Bromine is an essential trace element for assembly of collagen IV scaffolds in tissue development and architecture. Cell. 2014; 157:1380–1392. [PubMed: 24906154]
75. Friedl P, Alexander S. Cancer invasion and the microenvironment: plasticity and reciprocity. Cell. 2011; 147:992–1009. [PubMed: 22118458]
76. Filant J, Spencer TE. Endometrial glands are essential for blastocyst implantation and decidualization in the mouse uterus. Biol. Reprod. 2013; 88:93. [PubMed: 23407384]
77. Lejeune B, Van Hoeck J, Leroy F. Transmitter role of the luminal uterine epithelium in the induction of decidualization in rats. J. Reprod. Fertil. 1981; 61:235–240. [PubMed: 7452622]
78. Hohenester E, Yurchenco PD. Laminins in basement membrane assembly. Cell Adh. Migr. 2013; 7:56–63. [PubMed: 23076216]
79. Sasaki T, Fässler R, Hohenester E. Laminin: the crux of basement membrane assembly. J. Cell Biol. 2004; 164:959–963. [PubMed: 15037599]
80. Li R, Liang J, Ni S, Zhou T, Qing X, Li H, et al. A mesenchymal-to-epithelial transition initiates and is required for the nuclear reprogramming of mouse fibroblasts. Cell Stem Cell. 2010; 7:51–63. [PubMed: 20621050]
81. Zhang X-H, Liang X, Liang X-H, Wang T-S, Qi Q-R, Deng W-B, et al. The mesenchymal-epithelial transition during in vitro decidualization. Reprod. Sci. 2013; 20:354–360. [PubMed: 23302397]
82. Paria BC, Zhao X, Das SK, Dey SK, Yoshinaga K. Zonula occludens-1 and E-cadherin are coordinately expressed in the mouse uterus with the initiation of implantation and decidualization. Dev. Biol. 1999; 208:488–501. [PubMed: 10191061]
83. Reddi AH. Morphogenetic messages are in the extracellular matrix: biotechnology from bench to bedside. Biochem. Soc. Trans. 2000; 28:345–349. [PubMed: 10961916]
84. Lim H, Song H, Paria BC, Reese J, Das SK, Dey SK. Molecules in blastocyst implantation: uterine and embryonic perspectives. Vitam. Horm. 2002; 64:43–76. [PubMed: 11898397]

85. Paizis K, Kirkland G, Polihronis M, Katerelos M, Kanellis J, Power DA. Heparin-binding epidermal growth factor-like growth factor in experimental models of membranous and minimal change nephropathy. Kidney Int. 1998; 53:1162–1171. [PubMed: 9573530]

86. Tung HN, Parr MB, Parr EL. The permeability of the primary decidual zone in the rat uterus: an ultrastructural tracer and freeze-fracture study. Biol. Reprod. 1986; 35:1045–1058. [PubMed: 3814692]

87. Bany BM, Hamilton GS. Assessment of permeability barriers to macromolecules in the rodent endometrium at the onset of implantation. Methods Mol. Biol. 2011; 763:83–94. [PubMed: 21874445]

88. Yang H, Borg TK, Schmidt LP, Gao BZ. Laser cell-micropatterned pair of cardiomyocytes: the relationship between basement membrane development and gap junction maturation. Biofabrication. 2014; 6:45003.

89. Iwahashi M, Muragaki Y, Ooshima A, Nakano R. Decreased type IV collagen expression by human decidual tissues in spontaneous abortion. J. Clin. Endocrinol. Metab. 1996; 81:2925–2929. [PubMed: 8768853]

90. Roy S, Ha J, Trudeau K, Beglova E. Vascular basement membrane thickening in diabetic retinopathy. Curr. Eye Res. 2010; 35:1045–1056. [PubMed: 20929292]

91. Dempsey DA, Benowitz NL. Risks and benefits of nicotine to aid smoking cessation in pregnancy. Drug Saf. 2001; 24:277–322. [PubMed: 11330657]

92. Dockery P, Khalid J, Sarani Sa, Bulut HE, Warren Ma, Li TC, et al. Changes in basement membrane thickness in the human endometrium during the luteal phase of the menstrual cycle. Hum. Reprod. Update. 1998; 4:486–495. [PubMed: 10027600]

93. Huet YM, Dey SK. Role of early and late oestrogenic effects on implantation in the mouse. J. Reprod. Fertil. 1987; 81:453–458. [PubMed: 3323496]

94. Lei W, Ni H, Herington J, Reese J, Paria BC. Alkaline phosphatase protects lipopolysaccharide-induced early pregnancy defects in mice. PLoS One. 2015; 10:e0123243. [PubMed: 25910276]

95. Ninomiya Y, Kagawa M, Iyama K, Naito I, Kishiro Y, Seyer JM, et al. Differential expression of two basement membrane collagen genes, COL4A6 and COL4A5,demonstrated by immunofluorescence staining using peptide-specific monoclonal antibodies. J. Cell Biol. 1995; 130:1219–1229. [PubMed: 7657706]

96. Sado Y, Kagawa M, Kishiro Y, Sugihara K, Naito I, Seyer JM, et al. Establishment by the rat lymph node method of epitope-defined monoclonal antibodies recognizing the six different alpha chains of human type IV collagen. Histochem. Cell Biol. 1995; 104:267–275. [PubMed: 8548560]

97. Granero-Moltó F, Sarmah S, O'Rear L, Spagnoli A, Abrahamson D, Saus J, et al. Goodpasture antigen-binding protein and its spliced variant, ceramide transfer protein, have different functions in the modulation of apoptosis during zebrafish development. J. Biol. Chem. 2008; 283:20495–20504. [PubMed: 18424781]

98. Zhao X, Ma W, Das SK, Dey SK, Paria BC. Blastocyst H(2) receptor is the target for uterine histamine in implantation in the mouse. Development. 2000; 127:2643–2651. [PubMed: 10821762]

Highlights

- Peroxidasin is elevated during initiation of embryo-material interactions.
- Peroxidasin coincided with collagen IV and crosslinked uterine scaffolds.
- Location of GPBP coincided with laminin as uterine matrix thickened.
- Localization of peroxdasin and GPBP indicates them as BM toolkit proteins.
- Assembly dynamics suggest distinct roles of toolkit proteins in BM.

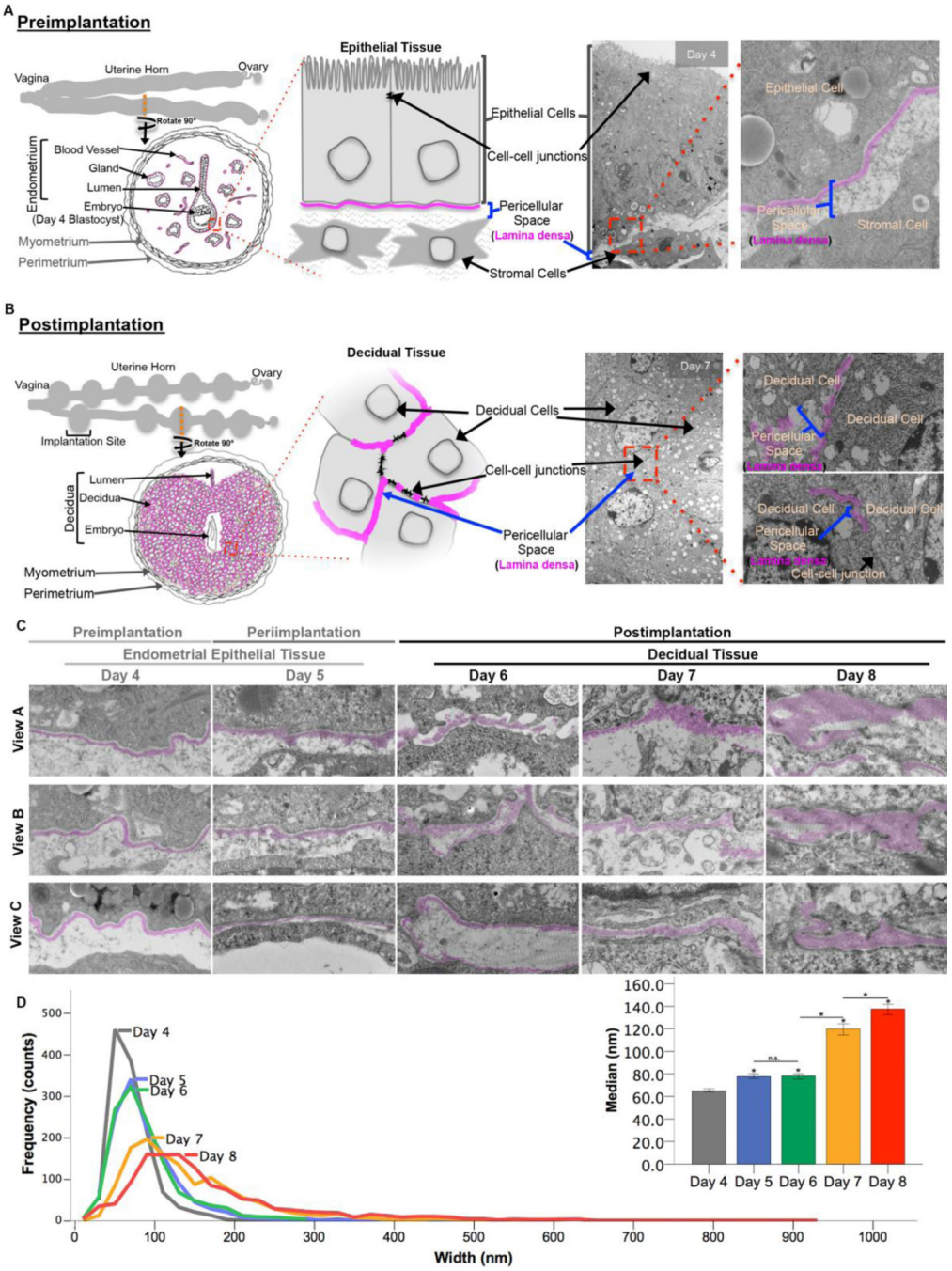

Figure 1.

Ultrastructure of basement membrane in the endometrium and deciduum during early pregnancy. Transmission electron microscopy of the mouse uterus from days 4–8 of pregnancy. Lamina densa (basement membrane) is highlighted with pink. **A**) Lamina densa of day 4 uterine endometrium with a diagram showing a cross-section of the uterine horn (orange dashed line), tissue anatomy, and the position of the lamina densa highlighted pink between the uterine epithelium and stroma; electron microscopic images at 9500x and 15000x. **B**) Lamina densa of day 7 decidua with a diagram showing a cross-section of

implantation site horn (orange dashed line), tissue anatomy, the position of the lamina densa highlighted pink within the deciduum; electron microscopic images at 9500x and 15000x). **C**) Micrographs (15000x) of the pericellular lamina densa from day 4–8 of pregnancy (views 1–3 represent the variation of the thickness of the lamina densa). **D**) Quantitation of lamina densa thickness. Frequency plot with lines representing distribution of widths out of 1300 measurements (counts) per day of pregnancy, and the same data as bars representing medians and 95% confidence intervals; Kruskal-Wallis test determined differences among groups (p-value < 0.001), and Post-hoc pairwise comparisons determined intergroup significance compared to day 4 of pregnancy and between sequential days (* p-value < 0.001, n.s. indicates no significant difference and p-value > 0.05).

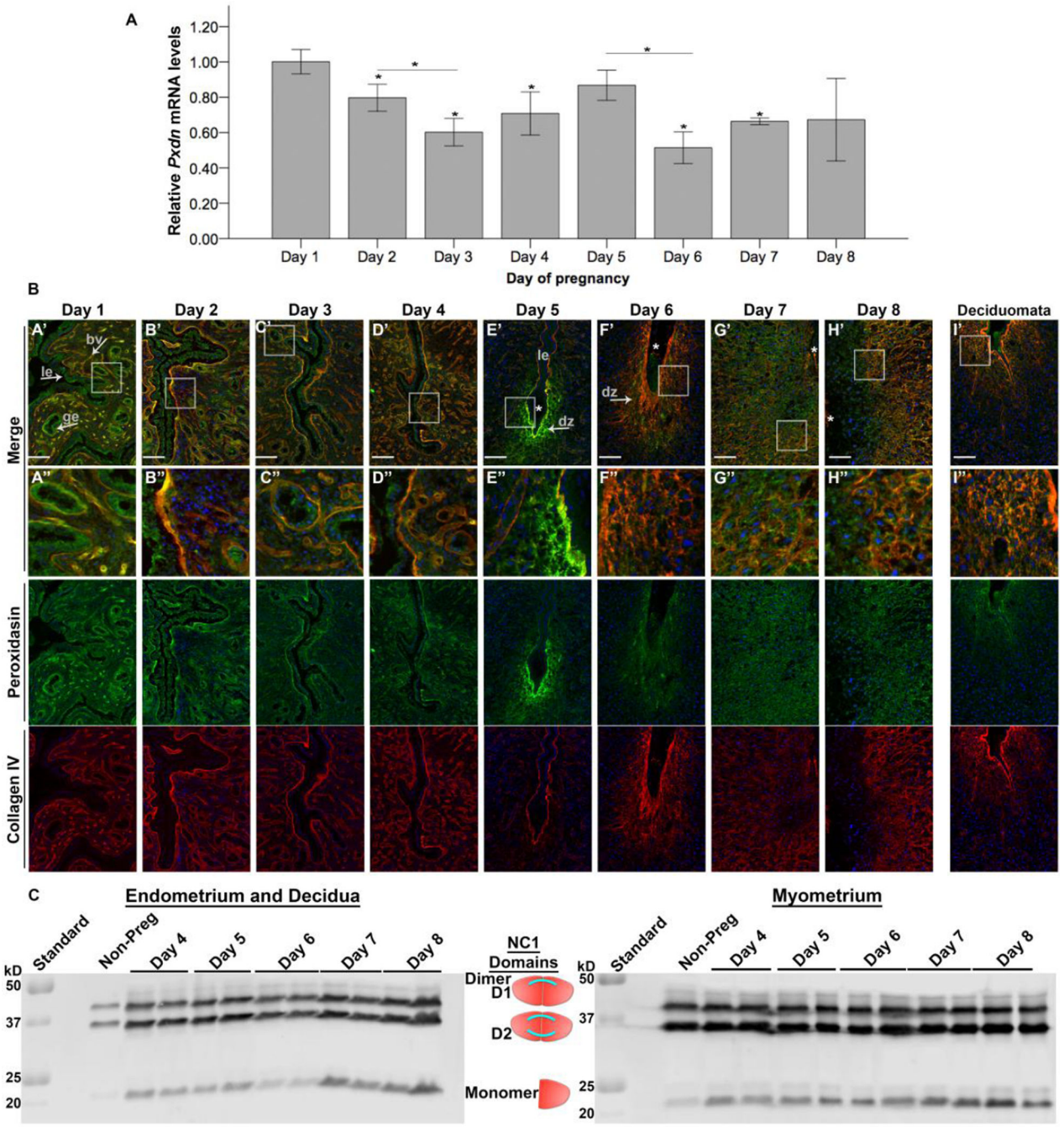

Figure 2.

Peroxidasin and collagen IV expression and localization during early pregnancy. **A**) Uterine mRNA expression of peroxidasin (*Pxdn*). Bars represent mean and ±SEM (* p-value ≤ 0.05). Comprehensive statistical comparisons and values are available in the supplement. **B**) Double immunofluorescence detection of collagen IV and peroxidasin in mouse uterus during early pregnancy. Images are oriented near the center of the uterus cross-section with collagen IV in red, peroxidasin in green, and nuclei in blue. Co-localization of collagen IV and peroxidasin is indicated by orange/yellow color. Asterisk (*) indicates the location of the

embryo. Scale bar= 100 μm. Inset (White Square; 140 μm^2 region) is a representative of the field showing merge of collagen IV and peroxidasin in the second row. Le, luminal epithelium; ge, glandular epithelium; bv, blood vessels; dz, decidual zone. **C**) Immunoblot of collagen IV NC1 domains for crosslinking analysis (non-pregnant (Non-Preg) and day 4- 8 endometrial explants and myometrium. Bands at approximately 37 kDa represent crosslinked NC1 domains, and bands at approximately 23 kDa represent monomeric NC1 domains.

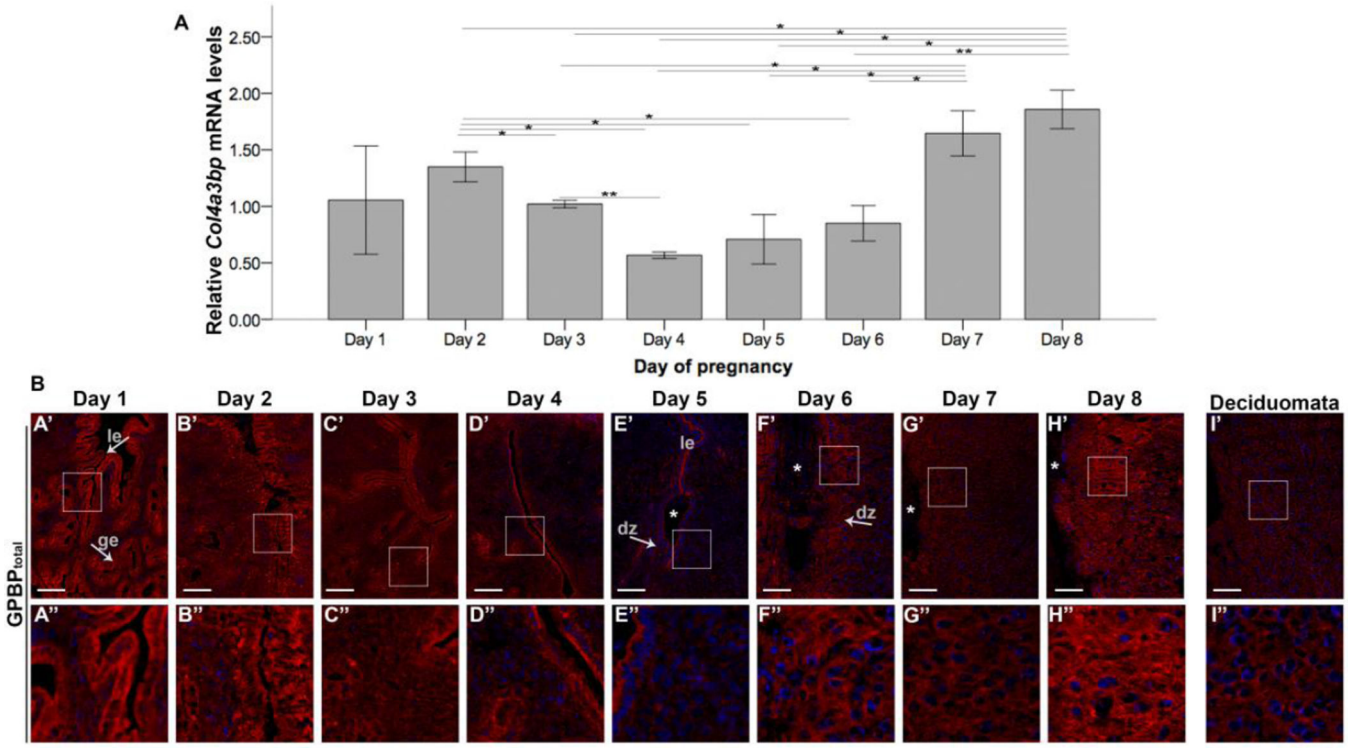

Figure 3.

Expression and localization of GPBP in the uterus during early pregnancy. **A**) Uterine mRNA expression of GPBP (Col4a3bp). Bars represent mean and ±SEM (* p-value ≤ 0.05, ** p-value ≤ 0.001). Comprehensive statistical comparisons and values are available in the supplement. **B**) Immunofluorescence detection of GPBP in mouse uterus during early pregnancy. Images are oriented near the center of the uterus cross-section with GPBP in red and nuclei in blue. Asterisk (*) indicates the location of the embryo. Scale bar= 100 μm. Inset (White Square; 140 μm^2 region) is a representative of the field showing localization of GPBP in the second row. Le, luminal epithelium; ge, glandular epithelium; bv, blood vessels; dz, decidual zone.

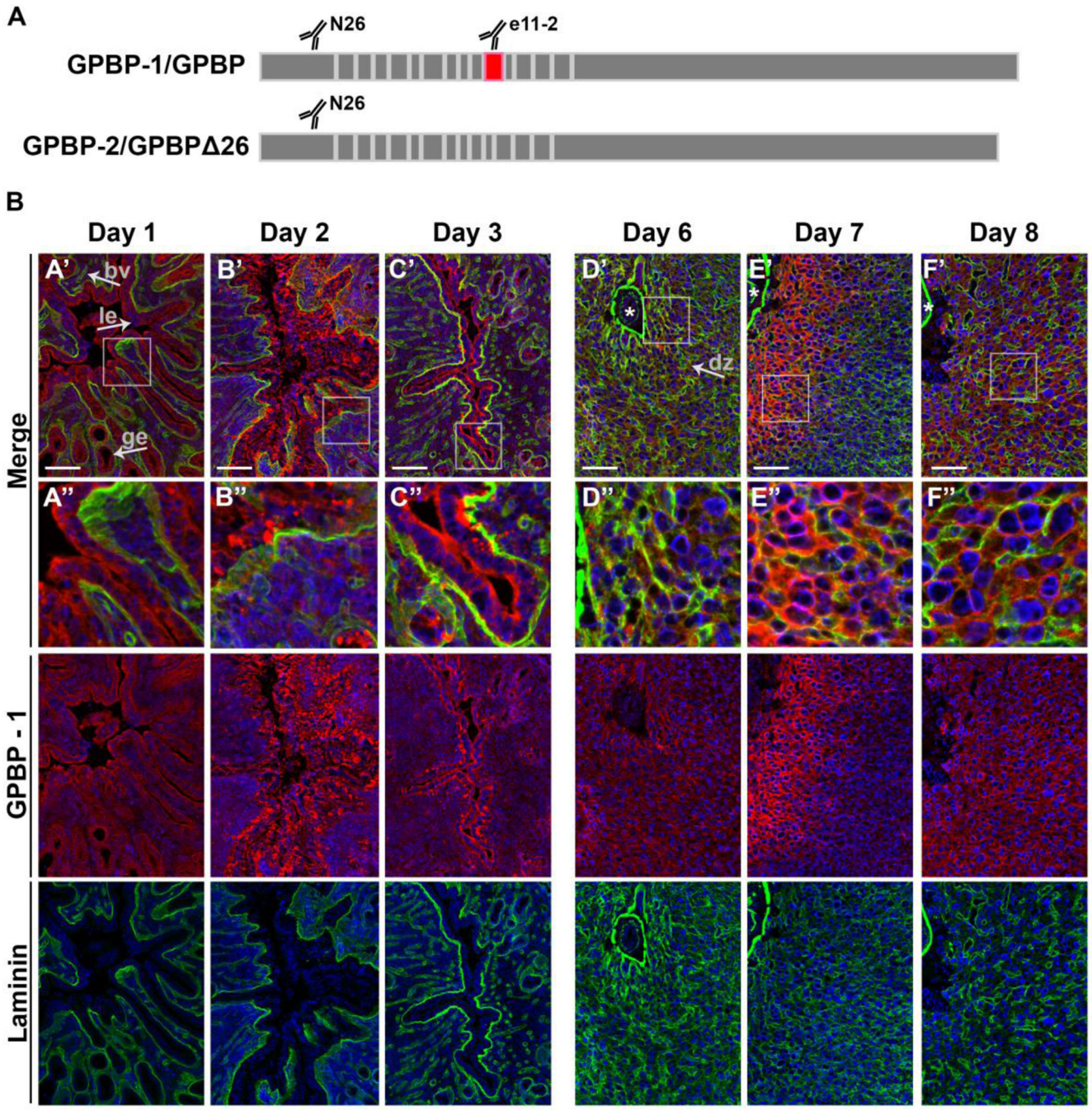

Figure 4.

Isoform GPBP-1 and laminin localization during early pregnancy. **A**) Diagram depicting areas of GPBP isoforms that mAb N26 and e11-2 specifically bind. The N26 antibody recognizes all isoforms of GPBP while the e11-2 antibody detects the 26-amino acid region that is encoded by exon 11 (shown as the red block), which is not present in GPBP-2 also called GPBPΔ26 or CERT. **B**) Double immunofluorescence detection of GPBP-1 and laminin in mouse uterus during early pregnancy. Images are oriented near the center of the uterus cross-section with GPBP-1 in red, laminin in green, and nuclei in blue. Co-

localization of GPBP-1 and laminin is indicated by orange/yellow color. Asterisk (*) indicates the location of the embryo. Scale bar= 100 μm. Inset (White Square; 140 μm^2 region) is a representative of the field showing merge of GPBP-1 and laminin in the second row. Le, luminal epithelium; ge, glandular epithelium; bv, blood vessels; dz, decidual zone.

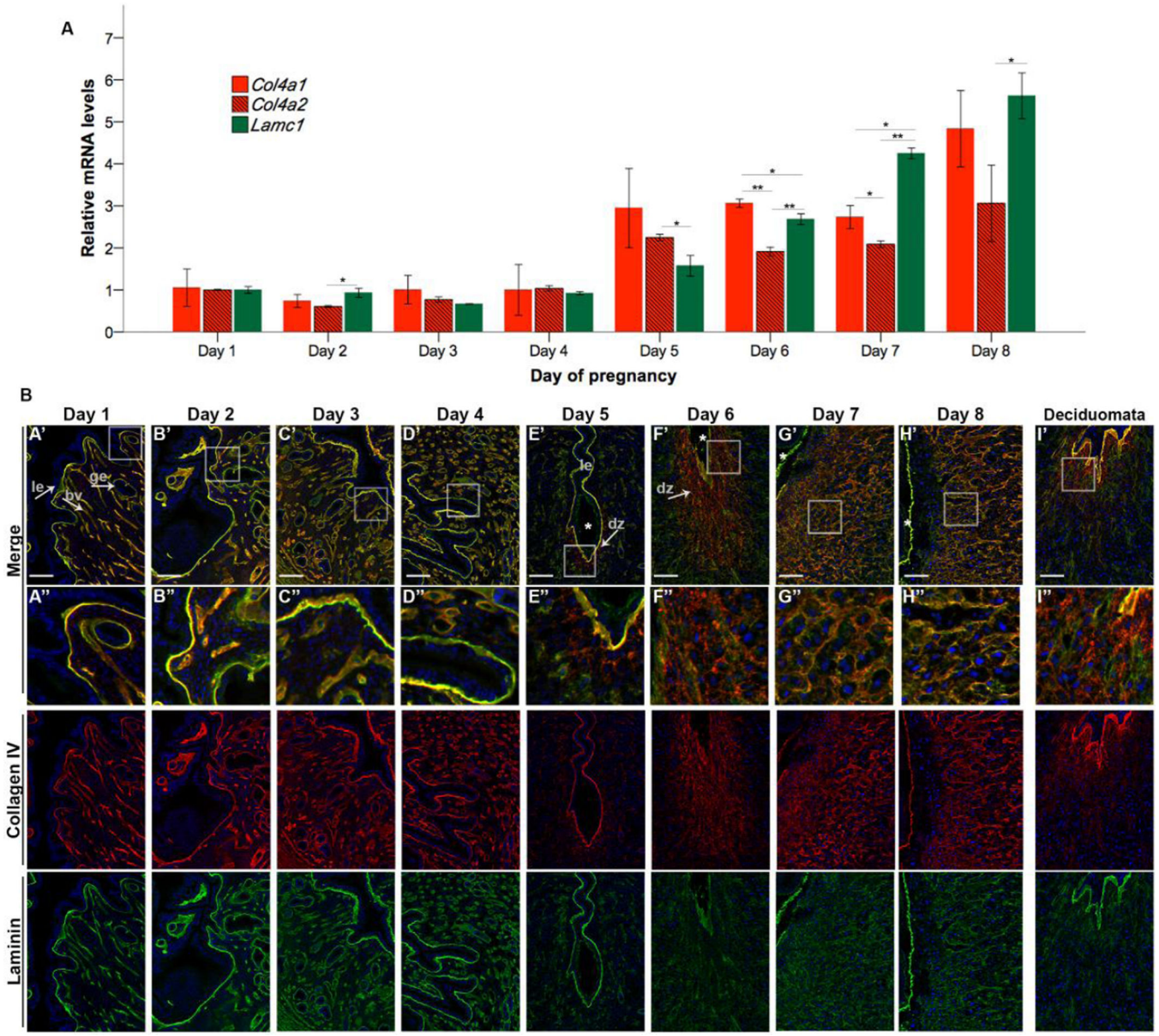

Figure 5.

Collagen IV and laminin expression and localization during early pregnancy. **A**) Uterine mRNA expression of collagen IV (*Col4a1* and *Col4a2*) and laminin (*Lamc1*). Bars represent mean and ±SEM (* p-value ≤ 0.05, ** p-value ≤ 0.001). Comprehensive statistical comparisons and values are available in the supplement. **B**) Double immunofluorescence detection of collagen IV and laminin in mouse uterus during early pregnancy. Images are oriented near the center of the uterus cross-section with collagen IV in red, laminin in green, and nuclei in blue. Co-localization of collagen IV and laminin is indicated by orange/yellow color. Asterisk (*) indicates the location of the embryo. Scale bar= 100 μm. Inset (White Square; 140 μm^2 region) is a representative of the field showing merge of collagen IV and laminin in the second row. Le, luminal epithelium; ge, glandular epithelium; bv, blood vessels; dz, decidual zone.

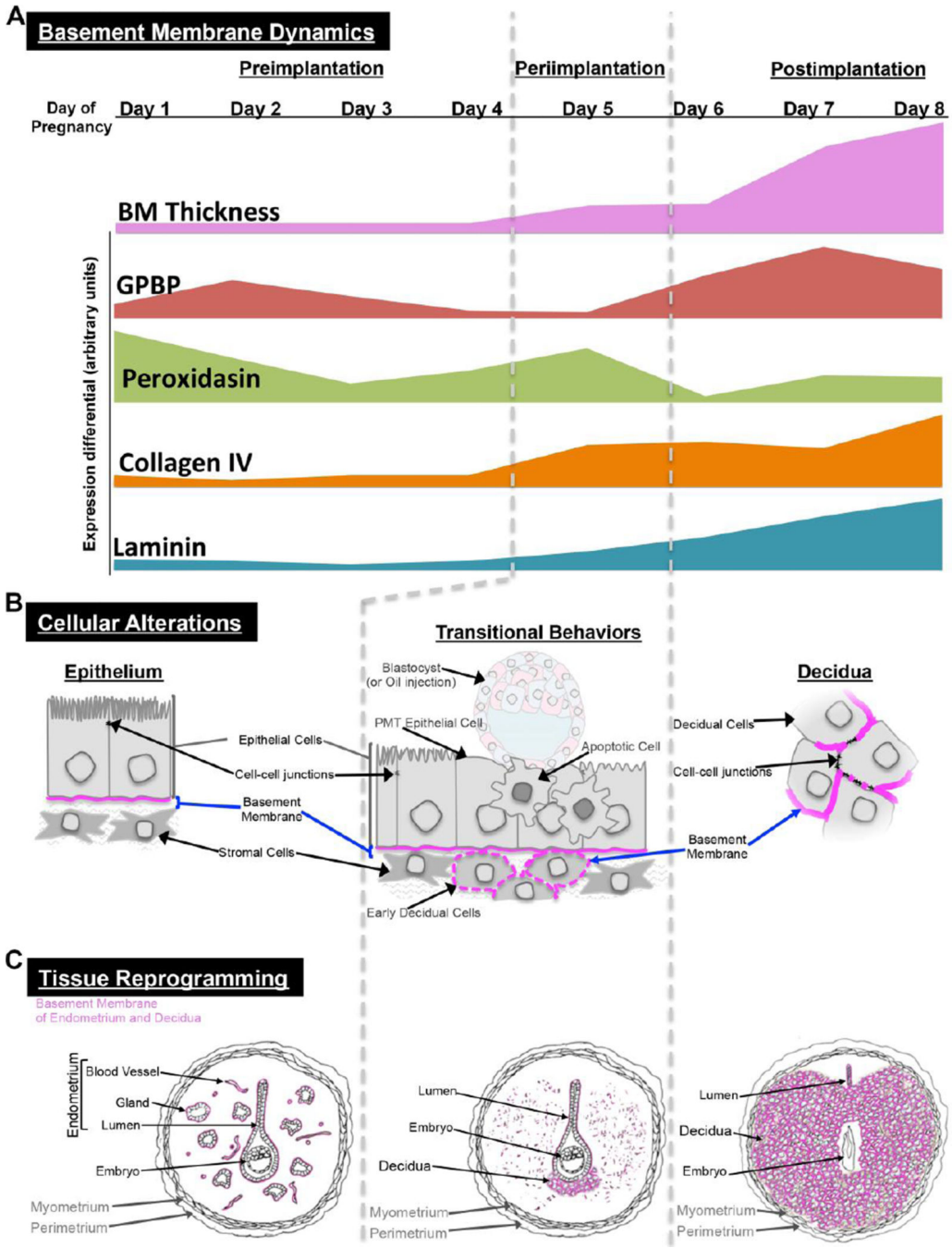

Figure 6.

Schematic model of BM toolkit and cellular dynamics during uterine tissue reprogramming for early pregnancy. Dynamics exhibited between days 1–4 for preimplantation, day 5 for periimplantation, and days 6–8 for post implantation. **A**) Basement membrane toolkit dynamics of ultrastructure thickening and mRNA expression changes (differential is relative for individual gene minimum and maximum expression levels throughout days 1–8 of pregnancy); fluctuations of expression levels are similarly mirrored in protein distribution. **B**) Cellular alterations incorporate different localization patterns of BM during the transition

from epithelium to decidua. PMT, plasma membrane transformation. **C**) Tissue reprogramming involves destruction and development of tissues supported by BMs, endometrium and decidua, respectively. Basement membrane represented by pink patterns. Dashed gray line demarcates BM toolkit, cellular, and tissue alterations that occur during periimplantation, also known as the window of implantation.

Table 1

Primer sequences used for qPCR.

Gene	Accession number	Primer sequence		Product size (base pairs)	Source/ Reference
Col4a1	NM_009931.2	Sense 5'-3 Antisense 5'-3'	CAG ATG ACC CAC TGT GTC CC ACC GCA CAC CTG CTA ATG AA	286	Primer Blast (NIH/ NCBI)
Col4a2	NM_009932.3	Sense 5'-3' Antisense 5'-3'	AGG ACC TAG GAC TGG CAG G GGG CAG TGG GGT ATA GAG GT	253	Primer Blast (NIH/ NCBI)
Col4a3bp	NM_001164222.1	Sense 5'-3' Antisense 5'-3'	CTT GCG TAG ACA TGG CTC AA CCC TCT GAA GCT CAT CCT TG	212	Primer Blast (NIH/ NCBI)
Lamc1	NM_010683.2	Sense 5'-3' Antisense 5'-3'	CAG CGA GAC CAC TGT GAA GT CGT CTC ACA GAA CTG TCC CC	262	Primer Blast (NIH/ NCBI)
Pxdn	NM_181395.2	Sense 5'-3 Antisense 5'-3'	GGC GGA AAG CAC TAA GTG TA GTT GCC GCC GTG AGA TTC	218	Primer Blast (NIH/ NCBI)
Rpl7	M29016	Sense 5'-3' Antisense 5'-3'	TCA ATG GAG TAA GCC CAA AG CAA GAG ACC GAG CAA TCA AG	246	Zhao et al. 2000 [98]